



RESEARCH ARTICLE

A hybrid indoor/outdoor detection approach for smartphone-based seamless positioning

Yuntian Brian Bai,*  Lucas Holden, Allison Kealy, Safoora Zaminpardaz,  and Suelynn Choy

School of Science, STEM College, RMIT University, Melbourne, Australia.

*Corresponding author. Yuntian Brian Bai, E-mail: yuntianbrian.bai@rmit.edu.au

Received: 3 November 2021; **Accepted:** 22 March 2022; **First published online:** 26 April 2022

Keywords: indoor and outdoor detection (IOD); wireless tracking; Wi-Fi- and smartphone-based positioning; signal-to-noise ratio (SNR) for IOD

Abstract

Indoor/Outdoor (IO) detection (IOD) using Wi-Fi- and smartphone-based technologies is in high demand and interest in both the industrial and research fields. This paper proposes a novel and effective hybrid IOD (HIOD) approach for detecting a smartphone user's IO location. The HIOD approach uses signals received from both Wi-Fi and GPS as well as the latest positioning technologies such as multilateration, fingerprinting and machine learning. This paper proposes and implements two-level signal-to-noise ratio (SNR) threshold parameters for the first time, which are specifically derived from GPS signals through 42 empirical tests at seven test sites with adequate environmental factors considered. Using the newly derived IOD threshold parameters and a set of IO detection rules, the HIOD approach is then tested at 20 test points (TPs) in a city canyon area, where most of the TPs are under semi-indoor or semi-outdoor conditions. The final test results show that a 100% IOD rate is achieved.

1. Introduction

The number of global smartphone users has reached 3.8 billion (May 2021), approaching half of the world's population (Deyan, 2021; Turner, 2021). This has led to a high demand for smartphone-based positioning applications, particularly since most people carry their smartphones on them throughout their daily activities. The popularity of smartphones has made Wi-Fi technology the single most popular wireless network protocol of the 21st century. In fact, Wi-Fi technology now powers most home and business wireless networks and public hotspot networks (Ta, 2018; Mitchell, 2019). The combination of Global Navigation Satellite System (GNSS) positioning (for outdoors) and Wi-Fi (for indoors) forms the basis of smartphone-based seamless positioning technology. This has become the dominant technology in location-based service (LBS) and other positioning application fields due to unprecedented innovation and demand from both research organisations and the commercial industry (Donovan, 2013; Machowinski, 2013; Mohapatra et al., 2014; Elkhodr et al., 2016; Mareco, 2018). In recent years, more and more positioning systems have started to use Wi-Fi instead of GNSS positioning in urban areas due to its free availability and ease of access. The free availability of Wi-Fi makes it even more popular in many urban canyons, where GNSS signals are wholly or partly blocked.

An effective indoor and outdoor positioning system fundamentally requires a robust strategic positioning method. Positioning methods such as the Cell of Origin (COO), multilateration and fingerprinting have become the three most popular and robust positioning methods in the past two decades. Each can

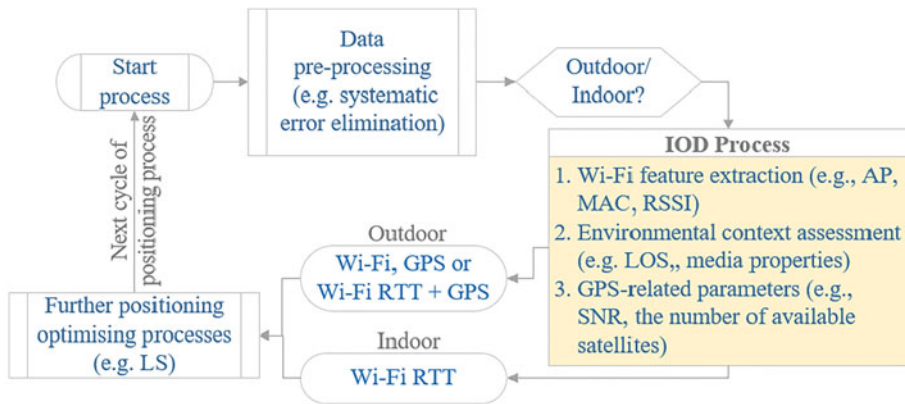


Figure 1. An example of the typical seamless (both indoor and outdoor) positioning process.

be selected according to specific environmental contexts such as (1) Line-Of-Sight (LOS) or None-Line-Of-Sight (NLOS) conditions; (2) the complexity of the environment; (3) the number of connected Access Points (APs) and (4) other device-related characteristics. Recently, the Time-of-Flight (TOF) has become a more accurate and robust ranging technique for Wi-Fi due to the release of the Fine-Time-Measurement (FTM) protocol in the IEEE 802.11mc wireless network standard (Yu et al., 2019; Bai et al., 2020). This protocol allows a smartphone user to use Wi-Fi Round-Trip-Time (RTT) technology for calculating the distance between an AP and a smartphone user. RTT significantly reduces the ranging error caused by radio signal fluctuations, and the positioning accuracy is therefore improved from approximately 5 m to a meter or sub-meter level, which is well matched with the positioning accuracy obtained from GNSS. This has promoted the integration of indoor and outdoor (IO) positioning techniques or the so-called *smartphone-based seamless positioning* (Diggelen et al., 2018). However, there still remains the challenging issue of distinguishing whether a smartphone user is located in an indoor or outdoor space so that the proper positioning algorithm can be applied accordingly (Okamoto and Chen, 2015; Zhu et al., 2019). For example, if the user is indoors, then Wi-Fi can be chosen as the positioning technology. Otherwise, in an outdoor setting, GNSS or a combination of GNSS and Wi-Fi needs to be selected as the positioning technology. More detailed descriptions of this concept are illustrated in Figure 1, where only GPS is applied hereafter although other GNSS constellations may also be valid either independently or jointly.

A critical requirement for the IOD is to find a set of feasible and robust criteria/algorithms that detect if an end-user is indoors or outdoors. In the real world, there are not only pure indoor and outdoor, but also semi-indoor and semi-outdoor environments. Yan et al. (2019) identified the four typical different environmental conditions:

- *Indoor space* – broadly, a physically enclosed space, such as a building or house, is referred to as an indoor space;
- *Outdoor space* – a space that is not entirely enclosed by walls, windows, doors, etc;
- *Semi-indoor space* – a space covered with a roof or canopy that is related to a building and combined with indoor and outdoor climate features, usually a GPS-denied space;
- *Semi-outdoor space* (or *semi-open space*) – a space that is not entirely enclosed, including human-made structures, which moderate the effects of outdoor conditions.

Real-world environments can be very complicated. However, once the IOD problem for semi-indoor and semi-outdoor spaces can be solved, it will be much easier for indoor and outdoor environments.

Previous IOD research has attempted to detect the IO status using the Received Signal Strength Indicator (RSSI) and built-in smartphone sensors such as the accelerometer, magnetometer and light

sensor (Li et al., 2014; Li et al., 2020). Some have adopted low power i-Beacon technology for IO detection (Zou et al., 2016). Chen et al. presented an IOD approach only using the number of available GPS satellites (Chen and Tan, 2017). Gao et al. described an IOD technique using 25 dB-Hz as a threshold of the carrier-power to the noise-density ratio (CNR: signal-to-noise ratio of a modulated signal) to distinguish the IO conditions (Gao and Groves, 2018). Other researchers have also explored light sensors, machine learning and sound-based reverberation patterns for the IOD process (Bhargava et al., 2014; Sung et al., 2015; Zhu et al., 2019). All these studies have shown that it is relatively easier to conduct the IOD process in a pure outdoor (or so-called open-air) or indoor space but much more challenging in semi-indoor and semi-outdoor areas (Gao and Groves, 2018; Zhu et al., 2019). In practice, none of the methods mentioned above are perfect for the IOD process under semi-indoor or semi-outdoor conditions.

This paper presents a hybrid IOD (HIOD) approach using Wi-Fi, GPS and smartphone technologies with careful consideration of the end-users environment. Devices and techniques such as Wi-Fi APs, RSSI, the number of connected APs or satellites and GPS Signal-to-Noise Ratio (SNR) are comprehensively investigated and tested for their suitability in the new approach. This includes an analysis of the RTT-based ranging estimations under the LOS and NLOS conditions. The rest of the paper is outlined as follows: in Section II, the positioning methods and specific technologies involved in this approach are introduced; then, the newly developed IOD approach is presented. Section III proposes two critical threshold parameters, the SNR_I and SNR_O parameters. Their empirical values are determined through 42 experimental tests at seven different sites. Section IV presents the details of testing and evaluation of the HIOD approach at ten outdoor Test Points (TPs) and ten indoor TPs. Conclusions and further work are presented in Section V.

2. Methodology

Several challenging urban canyon sites were selected for this research. Further, before investigating the HIOD approach, selection of the primary positioning methodology (that must be suitable for the environmental conditions) and appropriate positioning technologies were required. In this research, the RTT technology was selected for Wi-Fi-based range measurement (Bai et al., 2021; Gentner et al., 2020), which has been shown to be more straightforward for integration with GPS measurements. A common coordinate system for indoor and outdoor positioning must also be defined. Finally, the most suitable positioning optimisation algorithm that best integrates GPS and Wi-Fi signals must be identified. These considerations, plus a description of the final HIOD approach, will be introduced in the following sections.

2.1. Selecting a primary positioning method

Unless in exceptional cases, multilateration and fingerprinting are the two positioning methods generally selected for indoor positioning applications. Each has benefits and disadvantages in its application. Multilateration is suitable for a relatively open space, usually with a LOS condition between APs and the end user's smartphone. Research has shown that fingerprinting is a better choice for a stable complex space in which the multipath effect and NLOS condition occur (Pathak et al., 2014; Bai, 2016; Van Haute et al., 2016; Yaro et al., 2018). In this research, multilateration was selected as the positioning method due to the following reasons:

- a) relatively open spaces are often available in city canyon areas, which are more suitable for multilateration applications, although the NLOS condition exists for satellite signals detection;
- b) it is hard to conduct the training phase of the fingerprinting method in irregular and large outdoor spaces;
- c) there is a lack of variation of signal transmission in most outdoor spaces for adequately implementing a fingerprinting-based positioning system.

In practice, different strategic positioning methods and technologies are involved for different positioning scenarios. For example, Wi-Fi RTT-based trilateration is designated for indoor positioning in this project. For outdoors, either GPS alone, Wi-Fi alone or a combination of Wi-Fi and GPS can be involved for positioning. Figure 1 describes this strategy. As the figure shows, the determination of IOD assessment criteria is the main focus of this paper. Some fingerprinting concepts are also used to make the IOD assessment more robust.

2.2. Ranging with Wi-Fi RTT

Wi-Fi RTT technology provides a simple and accurate way of ranging calculation, especially in an open space. The round-trip-time and estimated range between a Wi-Fi AP and the end user’s smartphone (D_{est}) for a period of mean RTT can be obtained through Equations (1) and (2) (Yu et al., 2019):

$$t_{RTT} = \frac{1}{N} \left(\sum_{i=1}^N t_{4_i} - \sum_{i=1}^N t_{1_i} \right) - \frac{1}{N} \left(\sum_{i=1}^N t_{3_i} - \sum_{i=1}^N t_{2_i} \right) \tag{1}$$

$$D_{est} = \frac{1}{2} * t_{RTT} * c \tag{2}$$

where t_{RTT} is the round-trip-time of the signal transmitted between the smartphone and an AP; c is the signal transmission speed; t_{1_i} is the timestamp when the FTM framework was first sent by a Wi-Fi AP; t_{2_i} is the timestamp when the FTM signal arrives at the smartphone; t_{3_i} is the timestamp when the smartphone returns the acknowledgement signal to the AP; t_{4_i} is the timestamp when the acknowledgement signal is received by the AP; N is the successful burst number (where $N > 0, N < B$) and B is the total burst number (i.e., burst size, $B = 8$ as the default value in the Android operating system (OS)).

Generally, an Android Pie (Android P) or higher Android operating system is required for running the FTM. Other smartphone default settings such as the `ACCESS_FINE_LOCATION`, location tracking and Wi-Fi scanning permissions need to be enabled on the end-user device (Okamoto and Chen, 2015). All the estimated ranges are simplified to horizontal distances in this research. No vertical distance between an access point (AP) and a user is considered in this research (Gao et al., 2019).

2.3. Combination of the indoor and outdoor coordinate systems

A standard local coordinate system needs to be established for integrating both indoor and outdoor positioning processes seamlessly. First, an East, North and Up (ENU) local coordinate system is defined based on the universal Cartesian system. The ENU coordinates are formed from a plane tangent to the Earth surface fixed to a specific location, and hence it is sometimes known as a local tangent or local geodetic plane (see Figures 2 and 8).

For any point (e.g., $P(\phi, \lambda, h)$) received by a smartphone, its local ENU coordinates can be obtained from the point’s known latitude (ϕ), longitude (λ) and height (h). A local XYZ coordinate system is defined using the same initial point of the ENU system, which is for both indoors and outdoors. To simplify the testing process, only ‘EN’ and ‘XY’ coordinates are selected, while ‘Up’ and ‘Z’ coordinates are ignored. Assuming point $P(E', N')$ is a point with known universal Cartesian coordinates E' and N' (see Figure 2), then the coordinates can be converted geometrically to the local ENU and the local XYZ coordinate systems through Equations (4) and (5).

$$(\phi, \lambda, h) \Rightarrow (X_{ecef}, Y_{ecef}, Z_{ecef}) \Rightarrow (E', N', U') \Rightarrow (E, N, U) \tag{3}$$

The above coordinate transformations are accomplished by Equations (4)–(6); more details can be found in (Deakin and Hunter, 2013; PCG, P.C.o.G. and I.C.o.S.a.M.(ICSM), 2018; A Guide to

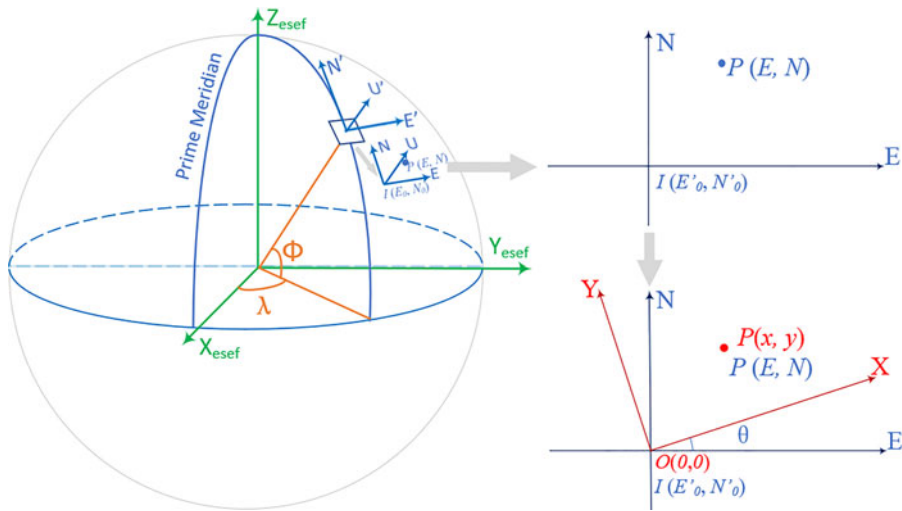


Figure 2. Relationships between the local ENU and the ECEF coordinate systems.

Coordinate Systems in Great Britain Geodesy & Positioning, 2020):

$$\begin{bmatrix} X_{ecef} \\ Y_{ecef} \\ Z_{ecef} \end{bmatrix} = \begin{bmatrix} (v + h)\cos\phi \cos\lambda \\ (v + h)\cos\phi \sin\lambda \\ [v(1 - e^2) + h]\sin\phi \end{bmatrix} \tag{4}$$

$$\begin{bmatrix} E' \\ N' \\ U' \end{bmatrix} = \begin{bmatrix} -\sin\lambda & \cos\lambda & 0 \\ -\sin\phi \cos\lambda & -\sin\phi \sin\lambda & \cos\phi \\ \cos\phi \cos\lambda & \cos\phi \sin\lambda & \sin\phi \end{bmatrix} \begin{bmatrix} X_{ecef} - X_{ref} \\ Y_{ecef} - Y_{ref} \\ Z_{ecef} - Z_{ref} \end{bmatrix} \tag{5}$$

where $v = (a/\sqrt{1 - e^2 \sin^2 \phi})$, $e^2 = 2f - f^2$ and $a = 6378137.0$ m is the semi-major axis of the earth based on the World Geodetic System 1984 (WGS84); f is the flattening and $1/f = 298.257223563$; $(X_{ecef}, Y_{ecef}, Z_{ecef})$ are the coordinates in the Earth-Centred, Earth-Fixed (ECEF) Cartesian coordinate system; $(X_{ref}, Y_{ref}, Z_{ref})$ are the ECEF coordinates of the origin of $E'N'U'$ coordinate system. Assuming the coordinates of the origin of the ENU coordinate system is (E'_0, N'_0, U'_0) in the $E'N'U'$ coordinate system, then

$$\begin{bmatrix} E \\ N \\ U \end{bmatrix} = \begin{bmatrix} E' - E'_0 \\ N' - N'_0 \\ U' - U'_0 \end{bmatrix} \tag{6}$$

$$\begin{bmatrix} x_G \\ y_G \end{bmatrix} = \begin{bmatrix} \cos\theta & \sin\theta \\ -\sin\theta & \cos\theta \end{bmatrix} \begin{bmatrix} E \\ N \end{bmatrix} \tag{7}$$

where x_G and y_G are the smartphone's GPS location measurements under the local XY coordinate system; E and N is the smartphone's GPS location measurement under the local EN coordinate system.

2.4. LS-based trilateration positioning process

Least-squares (LS) is a commonly used method for trilateration-based positioning, especially when a user is in motion or the motion parameters are untraceable. The coordinates obtained through the LS method are generally more accurate than those obtained by solving all equations algebraically (Gavin, 2020). Apart from the general LS application to Wi-Fi- and smartphone-based multilateration (see its implementation details in (Bai, 2016)), it can also be used in the multilateration positioning

process combining both GPS and Wi-Fi measurements. When such a combination is involved in the multilateration process, for example the combination of two Wi-Fi and one GPS measurements, the specific LS model becomes (with the assistance of Taylor series to the first-order expansion):

$$\begin{bmatrix} \frac{x_G - x_G^0}{d_{W1}^0} & \frac{y_G - y_G^0}{d_{W1}^0} \\ \vdots & \vdots \\ \frac{x_{wn} - x_0}{d_{Wn}^0} & \frac{y_{wn} - y_0}{d_{Wn}^0} \end{bmatrix} \begin{bmatrix} \Delta x \\ \Delta y \end{bmatrix} = \begin{bmatrix} d_G - d_G^0 \\ d_{W1} - d_{W1}^0 \\ \vdots \\ d_{wn} - d_{wn}^0 \end{bmatrix} \tag{8}$$

where

$$\begin{aligned} d_{Wi}^0 &= \sqrt{(x_{wi} - x_0)^2 + (y_{wi} - y_0)^2}; i = 1, \dots, n, \\ \Delta x &= x - x_0; \\ \Delta y &= y - y_0; \end{aligned}$$

where x and y are the smartphone’s coordinates in the local XY coordinate system, $d_{wi}(i = 1, \dots, n)$ is the measured distance between the i^{th} Wi-Fi AP and the smartphone, x_G and y_G are the smartphone’s GPS location measurements in the local XY coordinate system, and x_{wi} and $y_{wi} (i = 1, \dots, n)$ are the coordinates of the i^{th} Wi-Fi AP in the local XY coordinate system. The initial values of x_0 and y_0 can be obtained from other methods such as simplified LS, as described by Bai et al. (2020). The initial pair of x_G^0 and y_G^0 values can be assigned to x_0 and y_0 during the first round of iteration for a particular end user’s location.

Based on Equation (8), we define

$$dX = \begin{bmatrix} \Delta x \\ \Delta y \end{bmatrix}; B = \begin{bmatrix} \frac{x_G - x_G^0}{d_{W1}^0} & \frac{y_G - y_G^0}{d_{W1}^0} \\ \vdots & \vdots \\ \frac{x_{wn} - x_0}{d_{Wn}^0} & \frac{y_{wn} - y_0}{d_{Wn}^0} \end{bmatrix}; L = \begin{bmatrix} d_G - d_G^0 \\ d_{W1} - d_{W1}^0 \\ \vdots \\ d_{wn} - d_{wn}^0 \end{bmatrix}$$

The vector dX can be estimated using the LS method through Equation (9):

$$dX = (B^T B)^{-1} B^T L \tag{9}$$

The final estimated end user’s coordinates (\hat{x}, \hat{y}) can then be obtained from Equation (10) when the iteration is not required:

$$\begin{cases} \hat{x} = x_0 + \Delta x \\ \hat{y} = y_0 + \Delta y \end{cases} \tag{10}$$

2.5. Hybrid indoor and outdoor detection approach

As mentioned previously, successful IOD is critical for seamless smartphone-based positioning systems. This section proposes and describes an HIOD approach, which includes a combined use of Wi-Fi RSSI, Wi-Fi RTT-based range measurements, number of connected APs and number of interconnected satellites, as well as the SNR measurements and some valuable ideas from fingerprinting and machine learning. The hybrid approach includes three main rules ordered according to their reliability and

Table 1. Examples of the SNR values and their corresponding elevation values.

Satellite	Test 1		Test 2		Test 3	
	SNR (dB)	Ele (°)	SNR (dB)	Ele (°)	SNR (dB)	Ele (°)
G01					44.8	26.4
G08	17.3	39.0	18.7	33.6	40.4	30.1
G10	18.5	50.6	24.1	40.4	45.7	36.3
G21	16.2	27.2	18.8	42.1	45.4	48.1
G22			13.6	21.7	37.2	25.9
G23	16.6	22.6				
G27			16.7	25.2	29.3	19.8
G31			23.5	21.4	40.3	26.9
G32	18.6	83.3	20.0	72.8	45.1	66.4

effectiveness. The ultimate goal for all these rules is to find whether the smartphone user is located indoors or outdoors by evaluating the following:

- *Rule 1* – evaluating Wi-Fi-based ranges and RSSI values;
- *Rule 2* – evaluating the number of connected satellites and their SNR values;
- *Rule 3* – evaluating the number of connected APs, the numbers of available satellites and their corresponding SNR values, and comparing the current machine learning model (CML) and the latest machine-learning pattern (MLP).

Each of the rules has its own emphasis, and they are processed orderly during the IOD process. Rule 1 is the most straightforward rule, and it is processed first, followed by Rule 2, then Rule 3 (see [Figure 3](#)). Three critical parameters in the HIOD model need to be determined for successful IOD. One is a valid AP selection criterion, and the other two are the threshold values of SNR_I and SNR_O. Other parameters received from the end user's smartphone are also used during the IOD process, such as:

- the estimated Wi-Fi ranges, RSSI values and AP IDs from all connected APs, including the data received from those FTM-unsupported APs, which can be used for updating the MLP;
- the SNR values and IDs of all connected satellites;
- the number of connected APs and satellites (only GPS considered in this research).

A value of -71 dB is selected to be the RSSI threshold (RSS_T) for validating an AP as referred in (Bai, 2016). The MLP database is updated each time after Rule 1 or Rule 2 is processed. Previous research has also considered using the combination of SNR and elevation (i.e., SNR_Ele) values as an IOD criterion (Okamoto and Chen, 2015). In this research, the elevation was not selected for the following reasons:

- the orders of the SNR values and elevation values are not perfectly matched, and this leads to three confusing SNR, elevation and SNR*Elevation options for satellite selection;
- generally, a satellite with a higher elevation value also has a higher SNR value, although exceptional cases exist sometimes. Therefore, the SNR values already reflect the characteristics of signals from different satellite elevations;
- higher computational efficiency due to the reduced complexity with the usage of SNR only.

These scenarios are explained through the three testing results listed in [Table 1](#), where the orders for SNR, Elevation and SNR*Elevation are not exactly matched.

Thus, only SNR is selected for the HIOD model. [Figure 4](#) shows an example of the SNR values received by a smartphone, where nine satellites are detected and one SNR value per second is recorded for each satellite. Seven SNR curves are stable and have higher average values (the average SNR values

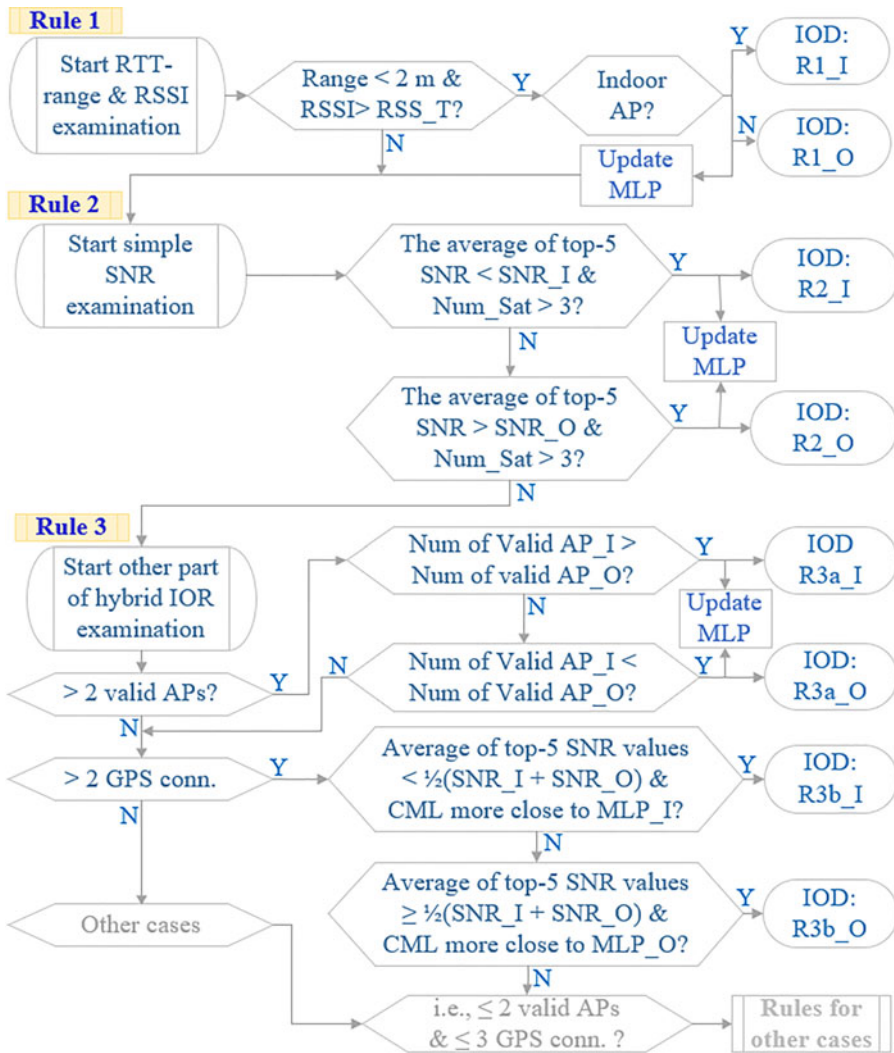


Figure 3. Principle of the HIOD approach.

are between 25 and 40 dB), whereas the other two are unstable and have lower average values (the average SNR values are between 21 and 25 dB). The testing results in Figure 4 match the real testing condition, where two satellites are partly blocked by the surrounding buildings; meanwhile, the top seven SNR curves demonstrate a smooth and stable trend even in a short period. These characteristics make the SNR values attractive for end-user’s IO detection.

As presented in Figure 3, a unique code for each type of detection path is necessary to represent a specific IOD result. The format of the unique code pattern is $R\#*_I/O$, where ‘R’ represents ‘Rule’; ‘#’ represents rule number; ‘*’ represents a subtype of a particular rule; ‘I’ means ‘indoor result’ and ‘O’ means ‘outdoor result’. Furthermore, two SNR threshold parameters (i.e., SNR_I and SNR_O) for IOD have been designated rather than one SNR threshold. One reason for defining two thresholds is that it is challenging for a single threshold parameter for successful IOD operation in semi-outdoor and semi-indoor environments (Gao and Groves, 2018; Zhu et al., 2019). Also, two SNR thresholds allow identification and removal of ambiguous cases and better clarify the whole IOD process. Another reason is to improve the detection rate. Two levels of thresholds practically provide more robust IOD results by using SNR_I as the ‘indoor threshold’ and SNR_O as the ‘outdoor threshold’. Based on the above

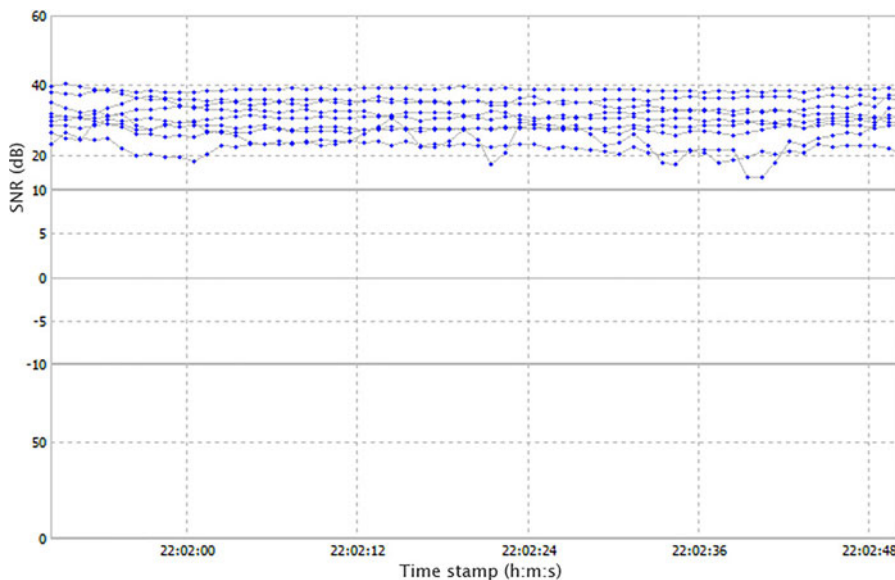


Figure 4. An example of SNR values received by a smartphone (approximately one-minute data collection period with nine satellites connected).

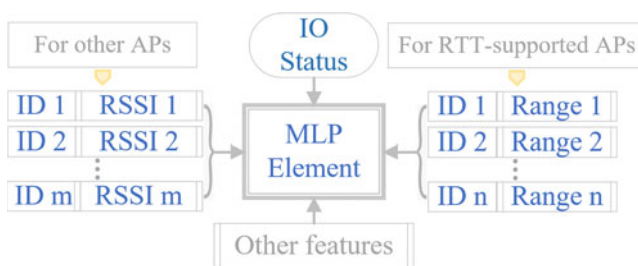


Figure 5. Key components of an MLP element.

clarification, a core issue for the success of the HIOD approach is how to determine appropriate SNR_I and SNR_O values. As a novel approach and without sufficient evidence for proving and assigning a specific value to each threshold, it was decided to obtain the SNR_I and SNR_O values through a range of empirical tests (introduced in Section III).

The main principle of the MLP model is derived from pattern recognition. A number of MLP elements are stored in the database and updated continuously during the HIOD process. A comparative analysis is undertaken when an unknown IO case occurs. Each MLP element includes a set of features extracted from the previous IOD process (see Figure 5). The following prerequisite conditions are applied for the feature of MLP element selection:

- 1) threshold – RSSI value ≥ -81 dBm (Bai, 2016);
- 2) a maximum of six RTT-supported APs and six other normal AP’s are collected. The range value is the selection criteria for RTT-supported APs, and the RSSI value is the criteria for normal APs.

3. Determination of the SNR_I and SNR_O values

It is essential to select diverse test sites to obtain convincing empirical results. Therefore, seven city canyon areas were selected (i.e., within the RMIT University city campus and Melbourne Central Train

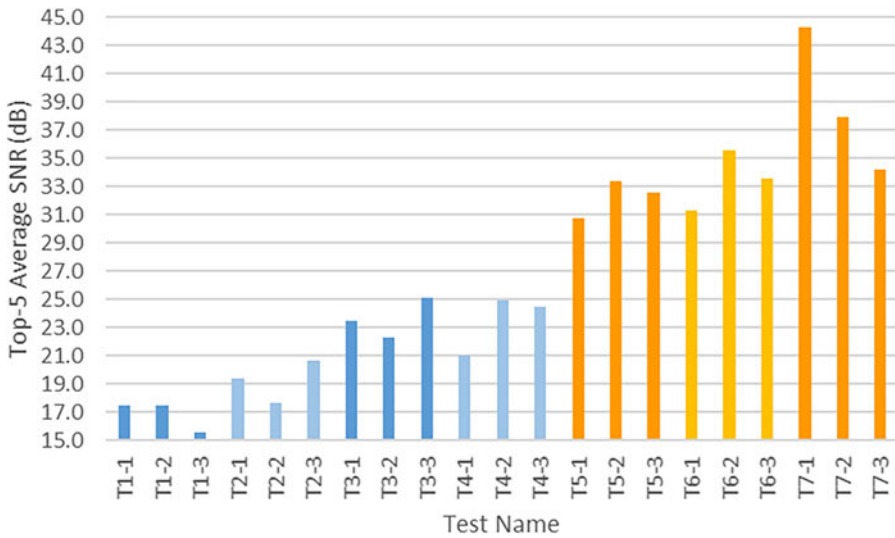


Figure 6. Comparison of the SNR values obtained from the empirical tests.

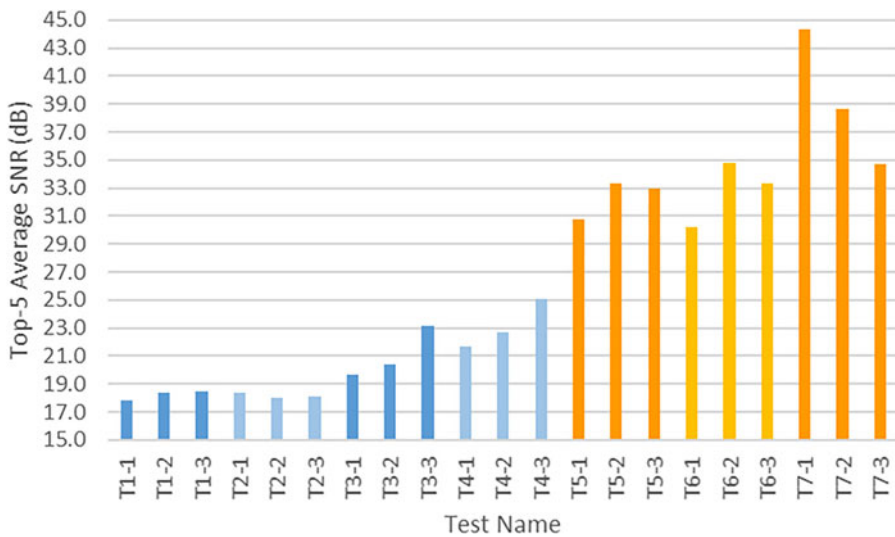



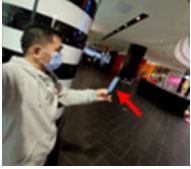




Figure 7. Comparison of the SNR values obtained from the repeated empirical tests.

Station in Melbourne) as specific testing sites. Five of the sites can be classified as semi-indoor or semi-outdoor conditions. Their details are described in Table 2 alongside two photos for each site. The first photo shows a broader site scene and the second shows a more focused location scene. The red arrow in each case points to the smartphone’s position. Three different local time periods were chosen for the tests, i.e., 10:30–11:30, 14:00–15:00 and 17:00–18:00. The empirical tests at each site were conducted in a specific period (approximately 1 min for each test). The preliminary test results from the first round of tests are summarised in Figure 6 and Table 3. A repeated round of empirical tests at each test site was also conducted. The test results are summarised accordingly in Figure 7 and Table 4. Thus, there were a total of six SNR results obtained from each TP after the two rounds of tests were completed.

A few highlighted points from Figures 6 and 7 are important and can be summarised as follows:

- 1) the SNR values from outdoors (see the orange bar charts) are higher than the SNR values from indoors (see the blue bar charts);

Table 2. *The seven testbeds selected for the empirical tests..*

No.	Site name	Description	Field type	Scene photo 1	Scene photo 2
1	MelCtrl 1	A large corridor within a concrete building; high pedestrian traffic.	Indoor		
2	MelCtrl 2	A corridor within an open entrance of a tall concrete building.	Semi-indoor		
3	RMIT 1	A large open office environment within a tall concrete building surrounded by windows.	Semi-indoor		

Continued.

Table 2. *Continued.*









No.	Site name	Description	Field type	Scene photo 1	Scene photo 2
4	RMIT 2	Beside RMIT 3, within a room with two open doors; a relatively open environment.	Semi-indoor		
5	MeICtrl 3	Beside a bus stop; 5 m to a tall building, surrounded by trees; a typical urban area.	Semi-outdoor		
6	RMIT 3	Beside RMIT 2, a platform on the top of a building on Level 7; surrounded by tall buildings on three sides (a city canyon area).	Semi-outdoor		
7	RMIT 4	A relatively open-air setting (behind the Old Gaol).	Outdoor		

Table 3. Preliminary SNR results from the empirical tests based on the seven different sites.

Satellite	MelCtrl 1			MelCtrl 1			RMIT 1			RMIT 2			MelCtrl 1			RMIT 3			RMIT 4		
	T1-1	T1-2	T1-3	T2-1	T2-2	T2-3	T3-1	T3-2	T3-3	T4-1	T4-2	T4-3	T5-1	T5-2	T5-3	T6-1	T6-2	T6-3	T7-1	T7-2	T7-3
G01												20.1	18.8	20.2		22.4	23.0		44.8	41.5	
G03		16.2	19.7		15.5	21.9		17.8	18.1		17.6	38.0		24.2	32.2		22.0	31.3		36.8	25.8
G04			17.9		15.6	16.6		17.8	24.8		20.5	19.7		19.9	34.7		38.4	42.5		38.8	37.8
G06								29.7							18.8						
G07			17.2						15.8			22.7			24.1			42.1			40.0
G08	17.3		16.8						15.7	18.7		20.8	19.5			25.3			40.4		30.0
G09			18.9						19.2		18.8	21.1		22.4	32.4		21.2	21.0		30.6	32.8
G10	18.5			19.3			28.1			24.1			42.4			28.6			45.7		
G16		16.0	21.1		18.7	23.3		18.5	33.1		31.3			22.8	39.5		38.5	27.0		31.4	28.5
G18																					
G21	16.2	16.7			16.2		17.5	15.9		18.8	18.4		24.1	30.5		29.4	24.1		45.4	26.5	
G22	9.7	16.7			18.6			15.8		13.6	25.1		19.8	40.2		22.6	40.8		37.2	38.2	
G23	16.6												16.3			19.7					
G24																					
G26		18.0	17.8		18.9			23.3			26.1	15.7		26.9	21.8		35.4	25.0		34.2	
G27									30.5	16.7			20.8		16.9	22.0		20.3	29.3		30.6
G30												14.2			22.4			17.2			28.7
G31		19.5					21.5	21.9		23.5	21.7		26.5	45.0		39.4	24.9		40.3	28.7	
G32	18.6	15.5		19.4			26.8			20.0			39.8			33.9			45.1		
No. Satellites	6	7	7	2	6	3	4	8	7	7	9	7	9	9	9	9	9	8	8	9	8
Top 5 Avrg.	17.4	17.4	15.5	19.4	17.6	20.6	23.5	22.2	25.1	21.0	24.9	24.5	30.7	33.4	32.6	31.3	35.6	33.6	44.3	37.9	34.2

Table 4. Preliminary SNR results from the repeated empirical tests based on the seven different sites.

Satellite	MelCtrl 1			MelCtrl 1			RMIT 1			RMIT 2			MelCtrl 1			RMIT 3			RMIT 4		
	T1-1	T1-2	T1-3	T2-1	T2-2	T2-3	T3-1	T3-2	T3-3	T4-1	T4-2	T4-3	T5-1	T5-2	T5-3	T6-1	T6-2	T6-3	T7-1	T7-2	T7-3
G01										15.5	21.9		18.7	22.4		20.8	22.4		41.1	44.9	
G03		17.2	19.7			20.9	15.7	18.4	17.3		17.4	32.8		25.1	32.2		24.9	37.2		34.1	27.6
G04		15.8	18.8			15.7		17.8	20.3		18.0	19.3		21.8	38.5		30.0	36.6		39.5	37.5
G06																					
G07			17.5						18.3			26.9		25.5			43.2				40.6
G08	15.6								16.8	14.4		26.9	18.8		21.6				40.9		
G09			17.3					17.7	19.7		19.2	19.5		24.2	31.7		23.2	25.0			33.6
G10	20.4			17.0			25.2			27.1			39.9			32.4				46.7	
G16		14.3	19.0			17.6		18.5	26.1		26.0			25.5	36.9		29.6	24.7			32.2
G18																					
G21	13.3	16.5					17.6			17.0	18.9		25.4	21.8		28.8	23.3		46.7	27.5	
G22		17.9	17.1				13.6			17.8	20.5		19.9	40.6		22.5	46.8		42.0	41.1	
G23	19.9												18.4			18.1					
G25		17.1																			
G26		16.8	15.1		19.6			22.7			25.0	17.2		34.1	21.6		40.0	22.9			32.9
G27									31.4	17.5		16.4	19.7		21.5	22.4		17.2	29.0		28.5
G30														19.0			18.5				39.2
G31		22.8			16.5		16.3	24.5		26.7	20.1		33.9	41.3		36.6	27.5		41.4	27.9	
G32	19.8			19.7			25.6			19.5			34.9			30.7				44.7	
No. Satellites	5	8	7	2	2	3	6	6	7	8	9	7	9	9	8	9	9	8	8	9	6
Top 5 Avrg.	17.8	18.4	18.5	18.4	18.1	18.1	19.7	20.4	23.2	21.7	22.7	25.1	30.8	33.3	33.0	30.2	34.8	33.3	44.3	38.6	34.7

- 2) the values from semi-indoor spaces are higher than the values from indoor spaces;
- 3) the SNR values from the semi-outdoor areas are lower than the value bars from an open space.

According to the above test results, a single SNR value may have higher uncertainty and not present the overall SNR level of the AP. For example, the SNR value from the G03-T4-3 test was 38 dB, much higher than the overall SNR level. This may mislead the IOD process. The average SNR values of three and five GPS connections were also compared, and the average of 5-SNR values was slightly more distinguishable than that of the 3-SNR values. Therefore, the average SNR value of five GPS connections was selected to assist in the SNR_I and SNR_O parameter determination. If the number of connected satellites is less than 5, the average SNR values of all the interconnected satellites is selected. With comprehensive analysis of the empirical results, and also considering the complexity of the semi-indoor conditions (e.g., an SNR value sometimes may be similar to a semi-outdoor SNR level when fewer obstructions exist), 25.0 dB and 33.0 dB were finally selected as the SNR_I and SNR_O values in this research. Nevertheless, the SNR_I and SNR_O values may be amended in the future when hardware and environmental factors are changed.

4. Experimental test and result discussion

4.1. Experimental IOD test

An experimental test was designated to examine the HIOD approach. The test site was selected from more than six different candidates of venues. The final test site was set up in the roof garden of Building 10, at the city campus of RMIT University, not typical but belonging to a mixed area of both semi-indoor and semi-outdoor. The test site is surrounded by tall buildings on three sides and also contains furniture and parterres here and there. The outdoor garden is under a semi-outdoor condition with parterres, benches and coffee tables. There is also an indoor room connected to the outdoor garden through a corridor. In [Figure 8](#), T1, T2, . . . T10 represent the ten outdoor TPs, and P1, P2, . . . P10 represent the ten indoor TPs. The major hardware devices used were six CompuLab WILD routers and a Pixel 3 smartphone. The duration of data collected at each TP was approximately 1 min using an Android-based APP developed in-house. All the APs and the smartphone were placed at a vertical distance of 1.72 m above the ground with known X and Y coordinates for each TP. The AP1, 2 and 3 were placed outdoors, and AP 4, 5 and 6 were mounted indoors. Referring to [Figure 8](#), all TPs were located in a semi-outdoor space; T1 through T7 were under a more complex environment, and T2 and T3 were in the worst outdoor condition for signal transmission. P3, P4, P5 and P6 can be considered to be in an indoor space, and the other indoor TPs were all in a semi-indoor space. Among those indoor TPs, as P1 and P7 were located very close to the open entrances, they were considered the hardest points for IO detection.

The SNR and Wi-Fi-based measurement results are summarised in [Tables 5](#) and [6](#), respectively. For the indoor TPs, the user's IO locations at P01, 03, 04, 06, 07, 08 and 10 were recognised by Rule 1, and at P02, 05 and 09 were recognised by Rule 2; for the outdoor TPs, the user's IO locations at T01, 04–09 were recognised by Rule 2, and at T02 and T03 were recognised by Rule 3, the IO location at T10 was recognised by Rule 1. All IO detection results from the 20 TPs are shown in [Table 7](#), and the correct detection rate was 100%.

4.2. Discussion

As shown in [Table 7](#), 70% of the indoor IO locations were recognised by Rule 1, and 30% were recognised by Rule 2. Conversely, 70% of the outdoor IO locations were recognised by Rule 2, 20% by Rule 3, and 10% by Rule 1. Compared to Rule 3, Rules 1 and 2 are computationally simpler but more robust. Fortunately, 90% of the IOD tasks were achieved by Rule 1 and Rule 2, which significantly reduced the processing time and improved the IOD efficiency without complicated calculations (see [Table 8](#)). [Table 8](#) also indicates that Rule 1 is generally the principal function for indoor detection, and Rule 2 is for outdoor detection, whereas exceptional cases often exist for those TPs under worse conditions. For

Table 5. SNR measurement results received from the 20 TPs.

Satellite	P01	P02	P03	P04	P05	P06	P07	P08	P09	P10	T01	T02	T03	T04	T05	T06	T07	T08	T09	T10
G01											35.7	27.3	20.8	21.6	22.3	19.0	18.5	20.5		
G03	36.1	27.6	21.3	20.7	20.6	28.9	27.8				21.7	19.4	24.8	27.9	37.5	36.4	30.6	42.1	34.4	36.3
G04	16.4	17.7	14.6	23.2	19.5	23.1	22.9	28.4	22.8	24.3	38.4	31.1	30.5	29.5	26.6	22.9	23.0	23.9	26.4	37.7
G05										14.4										
G06	14.5	12.2													21.7	22.7	26.3	26.5	21.6	18.0
G07	22.0	26.7	21.5	23.7	13.9	16.4	15.8	17.6	15.3	16.6							18.0	20.7	23.1	28.1
G08			12.9	17.9	16.1	22.0	21.1	28.1	22.7	22.0										
G09	17.5	15.2	14.1	16.0	13.4	19.1	23.0	36.8	20.0	24.5		17.4	21.0	15.9	17.3	21.0	35.0	34.1	26.0	28.4
G10																				
G14								16.5	16.0	20.9										
G16	22.4	19.4	17.0	13.8	21.7	19.2	18.9	19.2	19.0	12.8		33.0	33.5	35.5	39.0	36.9	39.1	38.5	38.1	33.6
G18																				
G21											38.3	28.9	19.6	20.4	20.0					
G22	31.0	28.2	18.4	21.4							42.7	39.8	30.0	44.2	38.5	36.9	42.5	33.0	32.1	30.7
G23																				
G24																				
G26	25.1	20.8	12.1	11.9							28.5	31.0	38.8	41.9	33.4	37.8	36.3	39.5	37.1	39.3
G27	13.2	17.1	13.7	14.3		14.9		30.3	22.0	23.6										
G28										13.6										
G30						13.4	15.3	16.3	18.7	17.0										
G31											40.1	23.6	28.1	26.3	27.9	38.7	35.7	34.2		
No. Satellites	9	9	9	9	6	8	7	8	8	10	7	9	9	9	10	9	10	10	8	8
Top 5 Avrg.	27.3	24.5	18.6	21.4	18.4	22.5	22.7	28.6	21.3	23.1	39.0	32.8	32.2	35.8	35.3	37.3	37.7	37.7	33.6	35.5

Table 6. Measurement results of the estimated distances and RSSI values from the 20 TPs.

TP	R(AP1)	RSSI	R(AP2)	RSSI	R(AP3)	RSSI	R(AP4)	RSSI	R(AP5)	RSSI	R(AP6)	RSSI
P01	8.86	-70					1.62	-55	6.66	-67	4.49	-69
P02			16.41	-86	12.59	-81	3.12	-58	7.86	-74	1.61	-59
P03	11.76	-72	17.39	-83	10.66	-80	4.75	-55	5.88	-68	-0.11	-52
P04			16.07	-83	9.26	-69	4.86	-60			0.71	-50
P05	12.31	-78			12.00	-79	4.43	-67	2.21	-67	2.41	-64
P06			13.36	-76			5.26	-58	0.05	-54	6.20	-66
P07			13.31	-80	4.37	-70	3.35	-59	0.53	-51	4.84	-65
P08	16.90	-89	13.81	-74	4.04	-68			1.44	-63	5.68	-61
P09	8.33	-84			8.77	-83			3.52	-68	5.07	-67
P10	9.47	-77			10.40	-80	0.12	-52	5.57	-61	3.88	-64
T01			11.63	-80	4.71	-70	14.93	-78	12.77	-89	17.76	-79
T02	9.42	-76			10.55	-78	4.68	-70	9.58	-81	6.47	-75
T03	3.73	-64					8.75	-82	12.12	-77	9.02	-74
T04	4.03	-72	14.70	-85	12.36	-77	10.81	-85			10.74	-76
T05			9.67	-70	10.17	-75			12.09	-77	11.87	-86
T06	2.18	-58			9.39	-82			14.12	-84		
T07	3.93	-69	5.79	-81	7.95	-78					11.90	-80
T08	6.10	-69	3.28	-64	7.52	-78			12.53	-84	12.50	-75
T09			2.16	-58					12.46	-87	14.34	-76
T10	7.35	-77	1.31	-63	7.34	-79	13.97	-83	16.27	-80	16.58	-86

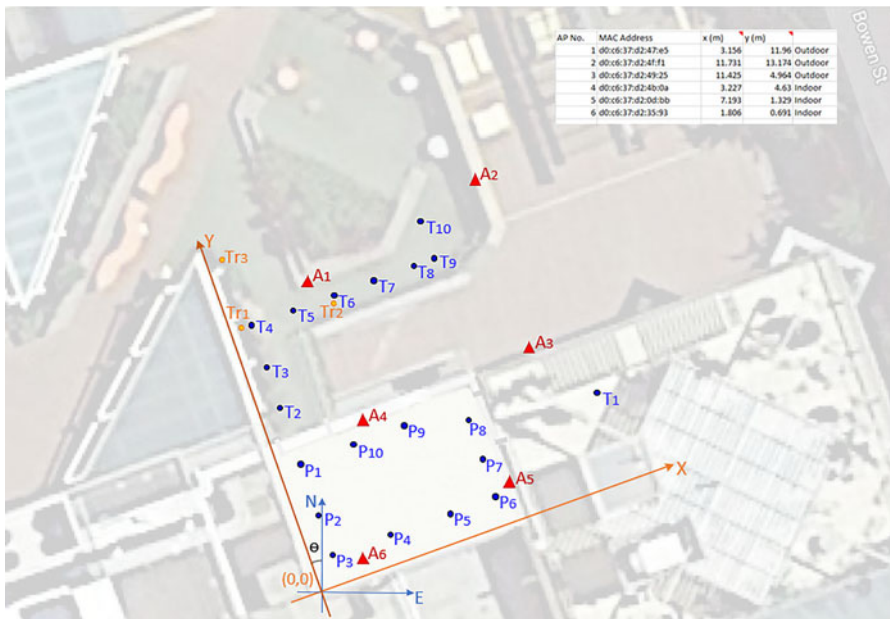


Figure 8. Sitemap of the test site and indoor and outdoor TPs.

Table 7. The final test results from HIOD.

Indoor TP	IOD result	Outdoor TP	IOD result
P01	R1_I	T01	R2_O
P02	R2_I	T02	R3b_O
P03	R1_I	T03	R3b_O
P04	R1_I	T04	R2_O
P05	R2_I	T05	R2_O
P06	R1_I	T06	R2_O
P07	R1_I	T07	R2_O
P08	R1_I	T08	R2_O
P09	R2_I	T09	R2_O
P10	R1_I	T10	R1_O

example, the HIOD processes at T2, T3 and P2 were not straightforward but required the involvement of additional rules.

5. Conclusions and further work

This paper presents a novel HIOD approach for recognising whether a smartphone user is located either indoors or outdoors through a set of rules. The HIOD approach provided a feasible and effective user IOD model using the available smartphone sensors, front-edge positioning and range estimation technologies. The HIOD approach mainly adopted the multilateration positioning method, and also considered the ideas from fingerprinting and machine learning. It not only used the latest Wi-Fi ranging measurement technology (i.e., the FTM technology) but also absorbed the essence of traditional Wi-Fi RSSI. Meanwhile, various surrounding environmental factors were also carefully considered, including a two-level SNR threshold concept proposed for the first time. In addition, the received Wi-Fi and GPS

Table 8. The HIOD occupation probabilities with Rules 1, 2 and 3.

	Rule 1	Rule 2	Rule 3
Indoor probability	70%	30%	0%
Outdoor probability	10%	70%	20%
Probability of Rules 1 & 2		90%	10%

signals were also organically integrated. The final experimental results showed that the HIOD approach achieved a 100% IO detection rate.

In the future, the HIOD approach will be further examined using more smartphones and under kinematic status.

Competing interests. None.

Acknowledgements. The authors want to thank Simon Fuller and Jenni Tomkinson for their support during the experimental tests.

References

- Bai, Y. B.** (2016). *Development of a Wi-Fi and RFID Based Indoor Location and Mobility Tracking System*. Melbourne, Australia: RMIT University.
- Bai, Y. B., Kealy, A. and Holden, L.** (2021). Evaluation and correction of smartphone-based fine time range measurements. *International Journal of Image and Data Fusion*, 12(3), 185–202.
- Bai, Y. B., Kealy, A., Retscher, G. and Holden, L.** (2020). A Comparative Evaluation of Wi-Fi RTT and GPS Based Positioning Sydney, Australia.
- Bhargava, P., Gramsky, N. and Agrawala, A.** (2014). Senseme: A System for Continuous, On-Device, and Multi-Dimensional Context and Activity Recognition. In *Proceedings of the 11th international conference on Mobile and ubiquitous systems: Computing*. Networking and Services.
- Chen, K. and Tan, G.** (2017). SatProbe: Low-Energy and Fast Indoor/Outdoor Detection Based on raw GPS Processing. In *IEEE INFOCOM 2017-IEEE Conference on Computer Communications*. IEEE.
- Deakin, R. E. and Hunter, M. N.** (2013). *Geometric Geodesy Part A*. Melbourne, Australia: Geospatial Science, RMIT University, 87–97.
- Deyan, G.** (2021). 67+ Revealing Smartphone Statistics for 2021. Techjury. Available from: <https://techjury.net/blog/smartphone-usage-statistics/#gref>
- Diggelen, F. V., Want, R. and Wang, W.** (2018). How to achieve 1-meter accuracy in android. In: *GPS World*, 3. Cleveland, OH: North Coast Media. Available from: <https://www.gpsworld.com/how-to-achieve-1-meter-accuracy-in-android/>.
- Donovan, F.** (2013). WLAN market to grow 57 percent by 2017. In: D. O. Group (ed.). *eeNews Europe*. Available from: <https://www.eenewsanalog.com/en/wlan-market-to-grow-57-percent-by-2017/>.
- Elkhodr, M., Shahrestani, S. and Cheung, H.** (2016). Emerging wireless technologies in the internet of things: A comparative study. *International Journal of Wireless & Mobile Networks (IJWMN)*, 8(5), 67–82.
- Gao, H. and Groves, P. D.** (2018). Environmental context detection for adaptive navigation using GNSS measurements from a smartphone. *NAVIGATION. Journal of the Institute of Navigation*, 65(1), 99–116.
- Gao, L., Tang, S. and Bai, Y. B.** (2019). *A New Approach for Wi-Fi-Based People Localisation in a Long Narrow Space*. *Wireless Communications and Mobile Computing*. Available from: <https://doi.org/10.1155/2019/9581401>.
- Gavin, H. P.** (2020). *The Levenberg-Marquardt Method for Nonlinear Least Squares Curve-Fitting Problems* Department of Civil and Environmental Engineering, Duke University 19. Available from: <https://people.duke.edu/~hpgavin/ce281/lm.pdf>.
- Gentner, C., Ulmschneider, M., Kuehner, I. and Dammann, A.** (2020). Wifi-rtt Indoor Positioning. In *2020 IEEE/ION Position, Location and Navigation Symposium (PLANS) (1029–1035)*. IEEE.
- Li, M., Zhou, P., Zheng, Y., Li, Z. and Shen, G.** (2014). IODetector: A generic service for indoor/outdoor detection. *ACM Transactions on Sensor Networks (TOSN)*, 11(2), 1–29.
- Li, S., Qin, Z., Song, H., Si, C., Sun, B., Yang, X. and Zhang, R.** (2020). A lightweight and aggregated system for indoor/outdoor detection using smart devices. *Future Generation Computer Systems*, 107, 988–997.
- Machowinski, M.** (2013). New high of \$4 billion for wireless LAN market in 2012. In: *Wireless LAN Equipment and Wi-Fi Phones*, Infonetics Research, California, USA, 5 March. Available from: <https://www.ciol.com/new-usd4-bn-wireless-lan-market-2012/>.
- Mareco, D.** (2018). *Wi-Fi Planning: Preparing for Growth in a Mobile-First World*. Charlotte, NC, USA: SecurEdge Networks. Available from: <https://www.securedgenetworks.com/blog/wi-fi-planning-preparing-for-growth-in-a-mobile-first-world>.

- Mitchell, B.** (2019). Introduction to Wi-Fi Wireless Networking. Lifewire (part of the Dotdash): 1500 Broadway, New York, NY 10036. p. 1–3.
- Mohapatra, S. K., Choudhury, R. R. and Das, P.** (2014). The future directions in evolving Wi-Fi: Technologies, applications and services. *International Journal of Next-Generation Networks (IJNGN)*, **6**(3), 13–22.
- Okamoto, M. and Chen, C.** (2015). Improving GPS-Based Indoor-Outdoor Detection with Moving Direction Information From Smartphone. In *UbiComp/ISWC'15 Adjunct: Adjunct Proceedings of the 2015 ACM International Joint Conference on Pervasive and Ubiquitous Computing and Proceedings of the 2015 ACM International Symposium on Wearable Computers*. The Association for Computing Machinery.
- OSGM15.** *A Guide to Coordinate Systems in Great Britain Geodesy & Positioning. Vol. 3.6.* (2020). Southampton, United Kingdom SO16 0AS: Ordnance Survey. Available from: <https://www.ordnancesurvey.co.uk/documents/resources/guide-coordinate-systems-great-britain.pdf>.
- Pathak, O., Palaskar, P., Palaskar, R. and Tawari, M.** (2014). Wi-Fi indoor positioning system based on RSSI measurements from Wi-Fi access points—a trilateration approach. *International Journal of Scientific & Engineering Research*, **5**(4), 1234–1238.
- PCG, P.C.o.G. and I.C.o.S.a.M. (ICSM).** (2018). *Geocentric Datum of Australia 2020 Technical Manual (Version 1.2)*. ANZLIC COMMITTEE ON SURVEYING & MAPPING (ICSM), 22–26.
- Sung, R., Jung, S.-h. and Han, D.** (2015). Sound based indoor and outdoor environment detection for seamless positioning handover. *ICT Express*, **1**(3), 106–109.
- Ta, V. C.** (2018). *Smartphone-based Indoor Positioning Using Wi-Fi, Inertial Sensors and Bluetooth (Doctoral dissertation, Hanoi University of sciences (Hanoi))*.
- Turner, A.** (2021). September 2021 Mobile User Statistics: Discover the Number of Phones in The World & Smartphone Penetration by Country or Region. Available from: <https://www.bankmycell.com/blog/how-many-phones-are-in-the-world>.
- Van Haute, T., De Poorter, E., Crombez, P., Lemic, F., Handziski, V., Wirström, N. and Moreman, I.** (2016). Performance analysis of multiple Indoor Positioning Systems in a healthcare environment. *International Journal of Health Geographics*, **15**(1), 1–15.
- Yan, J., Diakité, A. A. and Zlatanova, S.** (2019). A generic space definition framework to support seamless indoor/outdoor navigation systems. *Transactions in GIS*, **23**(6), 1273–1295.
- Yaro, A. S., Sha'ameri, A. Z. and Kamel, N.** (2018). Position estimation error performance model for a minimum configuration 3-D multilateration. *International Journal on Electrical Engineering and Informatics*, **10**(1), 153–169.
- Yu, Y., Chen, R., Chen, L., Guo, G., Ye, F. and Liu, Z.** (2019). A robust dead reckoning algorithm based on Wi-Fi FTM and multiple sensors. *Remote Sensing*, **11**(5), 504.
- Zhu, Y., Luo, H., Wang, Q., Zhao, F., Ning, B., Ke, Q. and Zhang, C.** (2019). A fast indoor/outdoor transition detection algorithm based on machine learning. *Sensors*, **19**(4), 786.
- Zou, H., Jiang, H., Luo, Y., Zhu, J., Lu, X. and Xie, Lx.** (2016). Bluedetect: An ibeacon-enabled scheme for accurate and energy-efficient indoor-outdoor detection and seamless location-based service. *Sensors*, **16**(2), 268.